ELSEVIER

Precambrian Research 77 (1996) 41–57

Precambrian Research

Late orogenic, plastic to brittle extension along the Robertson Lake shear zone: implications for the style of deep-crustal extension in the Grenville orogen, Canada

Jay P. Busch, Ben A. van der Pluijm

Department of Geological Sciences, 2534 C.C. Little Bldg., University of Michigan, Ann Arbor, MI 48109-1063, USA

Received 31 October 1994; revised version accepted 19 July 1995

Abstract

Rocks regionally metamorphosed and deformed at middle- to lower-crustal levels in the contraction-dominated Mesoproterozoic Grenville orogen are exposed in southern Ontario, Canada. Investigation of the Robertson Lake shear zone (RLSZ) indicates that extension is a significant component in the late tectonic evolution of this deeply eroded orogen. The RLSZ is a discrete zone 0.5–1.0 km thick that can be traced for nearly 100 km, cross-cutting regional structures and lithologic units. The zone is composed of a thick mylonite zone and a narrow overlying brecciated zone. Mylonite foliation shallowly dips east-southeast and contains a down-dip lineation. Mylonites are characterized by microstructures indicative of crystal-plastic deformation and contain a variety of shear-sense indicators, including S–C and C–C′ composite fabrics, sigma porphyroclasts, mica fish and other shape fabrics oblique to shear planes, consistently indicating a normal (down-to-the-east) sense of shear. A zone of cataclastic structures overlies the mylonite zone, and brittle deformation overprints the mylonitic fabrics. Slickensides in the zone generally strike parallel to foliation in the mylonites but have steeper dips. Sense of slip indicators and brittle fault orientations also indicate down-to-the-east displacement during east–west extension. Juxtaposition of brittle and crystal-plastic structures is resolved with a model of displacement during exhumation whereby localization of cataclasis occurred along a previously active mylonite zone. Metamorphic facies are upper greenschist in the hanging wall and upper amphibolite in the footwall and metamorphic grade increases from west to east in both the hanging wall and footwall. The regional variations in metamorphic grade and the low-angle shear zone geometry are a result of isostatic flexural rotations that accompanied extension. Combined with the crystal-plastic to cataclastic nature of the RLSZ, new $^{40}Ar/^{39}Ar$ isotope data from biotite constrain the timing of shear zone displacement until at least 901 ± 1 Ma, late in the evolution of the Grenville orogen.

1. Introduction

Structures in the Grenville Province of North America are generally considered to be a lower- to mid-crustal expression of Mesoproterozoic thrust tectonics (Davidson, 1984; Hanmer, 1988; Rivers et al., 1989; McEachern and van Breemen, 1993). Recently, extensional deformation closely associated with the last phase of the Grenville orogenic cycle has also been recognized (Hanmer, 1988; van der Pluijm and Carlson, 1989; Carlson et al., 1990; Mezger et al., 1991; Culshaw et al., 1994). This study demonstrates the importance of late orogenic (post-metamorphic) extension in the Grenville orogen. To understand the tectonic evolution of the Grenville orogen, and the assembly of deep-crustal terranes in general, data on terrane and domain boundaries must be obtained (e.g. van der Pluijm et al., 1994). In this paper the term domain is used to describe an assemblage of rocks with

SSDI 0301-9268(95)00044-5

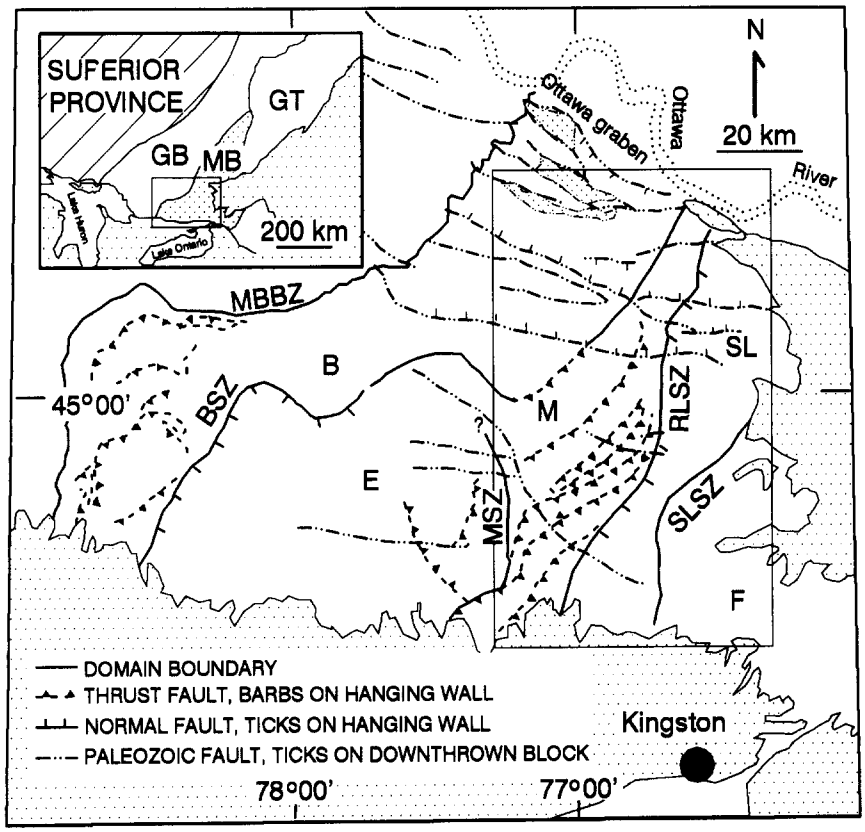

Fig. 1. General subdivisions of the Grenville orogen, domains and major structures of the Metasedimentary Belt (modified from Ontario Geological Survey map 2578, 1992a, b). Abbreviations are: *B* = Bancroft domain; *E* = Elzevir domain; *M* = Mazinaw domain; *SL* = Sharbot Lake domain; *F* = Frontenac domain; *MBBZ* = Metasedimentary Belt boundary zone; *BSZ* = Bancroft shear zone; *MSZ* = Moorton shear zone; *RLSZ* = Robertson Lake shear zone; *SLSZ* = Sharbot Lake shear zone. Light stipple is Paleozoic cover. Inset shows location of map area with: *GB* = Gneiss belt; *GT* = Granulite terrane; *MB* = Metasedimentary Belt (dense stipple). Box is the location of maps in Fig. 2.

distinct lithologic, metamorphic, or geophysical characteristics, but does not necessarily imply a genetic distinction. The term terrane is used to describe an assemblage of rocks with a clearly different tectonic and metamorphic history than neighboring regions. It is important to establish whether domain boundaries offset regional metamorphic patterns, cross-cut plutonic complexes and large-scale regional structures, and are zones of displacement. This paper focuses on one boundary, the Robertson Lake shear zone (RLSZ), which separates two domains within the eastern Metasedimentary Belt (Fig. 1). The purpose of this paper is to report field and microstructural observations that document the RLSZ as a late orogenic normal-sense shear zone, which was active over the transition from crystal-plastic to cataclastic deformation during exhumation. New $^{40}Ar/^{39}Ar$ data from biotite, regional metamorphic data, and structural observations place constraints on the temporal and geometric evolution of continental extensional tectonics in the Grenville orogen.

The RLSZ was first recognized by Smith (1958). The mapping programs of the Ontario Geological Survey have compiled several detailed maps that define the outcrop trace of parts of the RLSZ (Wolff, 1982, 1985; Easton, 1988a; Pauk, 1989a, b). The zone has been defined as an east-southeast dipping crystal-plastic mylonite zone with locally intense cataclastic deformation (Jackson, 1980; Carter, 1981; Easton, 1988a, b). Several studies have reported normal slip-sense indicators along brittle faults within the RLSZ (Wolff, 1985; Pauk, 1989a, b). Easton (1988c) recognized the regional extent of the RLSZ and the contrast in metamorphic facies and lithologies on either side of the

zone. Cosca et al. (1991, 1992) found a discontinuity in hornblende $^{40}Ar/^{39}Ar$ cooling ages (~70 m.y.) across the RLSZ and based on $^{40}Ar/^{39}Ar$ cooling ages concluded that extension may have occurred along all major tectonic boundaries within the Metasedimentary Belt by ~900 Ma. Mezger et al. (1993) showed that the RLSZ is a major tectonic boundary and may be a suture separating the Sharbot Lake domain from the Mazinaw domain. However, detailed field relations and structural information such as mylonite shear-sense were not available at that time.

2. Regional geology

The RLSZ lies within the Metasedimentary Belt of the Grenville orogen (Fig. 1). The Metasedimentary Belt is composed of marble, clastic metasedimentary rocks, and a variety of plutonic and volcanic rocks. The Metasedimentary Belt has been divided into five lithotectonic domains based on geophysical, lithologic and chronologic data (Easton, 1992). The RLSZ separates the Sharbot Lake and Mazinaw domains. The Mazinaw domain is dominated by deformed felsic and alkalic plutonic rocks, clastic metasedimentary rocks (quartzofeldspathic schist, gneiss and mica schist), and metavolcanic rocks (amphibole schist) metamorphosed at upper greenschist to upper amphibolite-facies conditions with metamorphic grade increasing from west to east (Fig. 2a) (Hutcheon and Moore, 1973; Sethuraman and Moore, 1973; Carmichael et al., 1978). The oldest rocks of the Mazinaw domain have crystallization ages between 1185 and 1270 Ma (Bell and Blen-

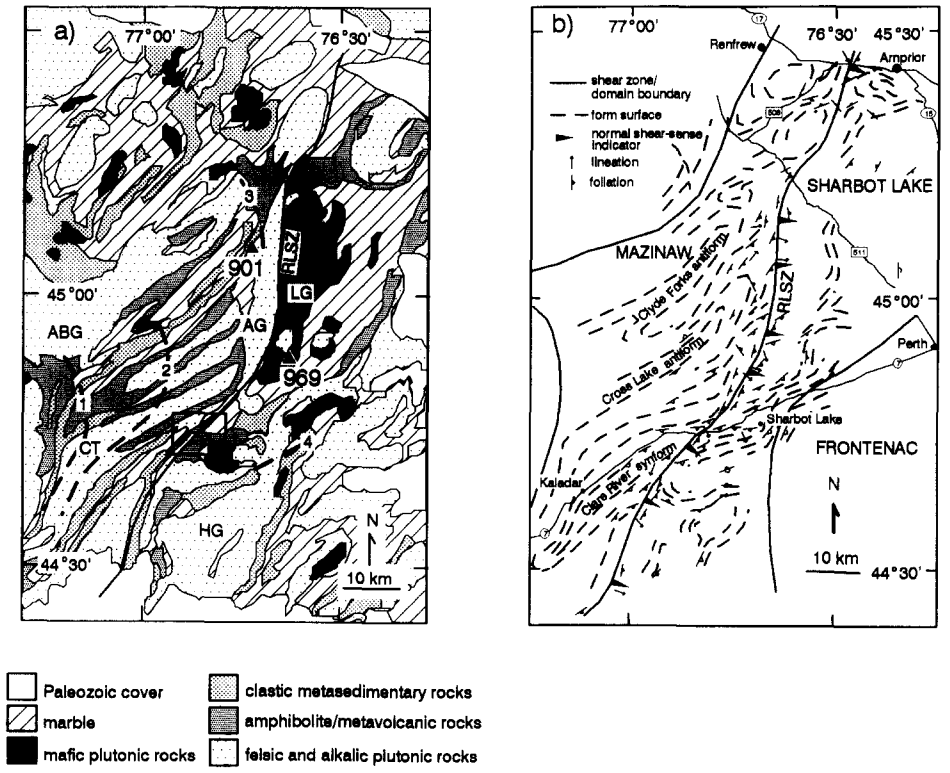

Fig. 2. (a) Geologic map (modified from Ontario Geological Survey map 2544, 1992a, b) with isograds (dashed lines) and thermochronologic data. Isograds are: 1 = garnet + muscovite + chlorite = staurolite + biotite + quartz; 2 = kyanite = sillimanite; 3 = muscovite + plagioclase + quartz = sillimanite + K-feldspar; 4 = garnet + hornblende + quartz = pyroxene + plagioclase, with higher grades toward the east and southeast (from Carmichael et al., 1978). Triangles are $^{40}Ar/^{39}Ar$ biotite cooling ages from this study (from Fig. 8). Box shows area of Fig. 4a. Abbreviations are: *LG* = Lavant gabbro; *HG* = Hinchinbrooke gneiss; *AG* = Addington granite; *CT* = Cross Lake tonalite; *ABG* = Abinger granite. (b) Regional gneissosity form-surface map of the study area showing the general east-northeast trend of major structures slightly oblique to the RLSZ and locations of field and micro-scale normal shear-sense indicators. Based on mapping by the authors and data from Wolf (1982, 1985) and Pauk (1989a, b).

kinsop, 1980; van Breemen and Davidson, 1988; Lumbers et al., 1990; Corfu and Easton, 1995). The overlying Flinton Group clastic metasedimentary rocks, marble and metavolcanic rocks, were originally deposited after 1150 Ma (Sager-Kinsman and Parrish, 1993). Three metamorphic events probably associated with accretion of the Metasedimentary Belt to the Gneiss Belt (~ 1190 Ma), collisional reactivation of the Metasedimentary Belt boundary zone (1080–1060 Ma) and a later event with associated synorogenic extension (995–1050 Ma) affected the rocks of the Mazinaw domain (Easton, 1992; Corfu and Easton, 1995; McEachern and van Breemen, 1993; Mezger et al., 1991; Mezger et al., 1993). Regional structures of the Mazinaw domain are expressed as doubly plunging refolded isoclinal folds (Moore and Thompson, 1980; Ford, 1992). These structures are evident in east-northeast trending folds such as the Clyde Forks and Cross Lake antiforms and the Clare River synform defined by lensoid plutonic bodies and overlying metasedimentary sequences (Figs. 2b). In summary, the Mazinaw domain has experienced multiple Mesoproterozoic tectonic events resulting in regional east-northeast trending folds, thrust faults, and greenschist to upper amphibolite-facies metamorphism.

The Sharbot Lake domain is dominated by mafic and intermediate meta-igneous rock and marble (Fig. 2a). Marble is generally light blue and white, banded and coarse-grained in the central and eastern portions of the domain. Marbles are finer-grained, darker-colored and preserve bedding near the RLSZ. Metavolcanic rocks are veined (epidote, calcite) epidote-amphibolites with chlorite alteration and primary volcanic features near the RLSZ (Easton, 1992). To the east, away from the RLSZ, metavolcanic rocks are coarse crystalloblastic garnet-amphibole schists and gneisses. The most extensively exposed plutonic complex, the Lavant gabbro has a U/Pb zircon date of 1225 Ma (Corfu and Easton, 1994) and is hydrothermally altered and deformed along its western margin adjacent to the RLSZ. Quantitative thermobarometric data are lacking in the Sharbot Lake domain but based on preservation of primary structures, metamorphic textures and assemblages, the metamorphic grade increases to the south and east (Carmichael et al., 1978; Easton, 1988b, 1992). An isolated U/Pb sphene date of 1152 Ma, interpreted as a metamorphic growth age, has been reported by Mezger et al. (1993). Crystallization ages inferred from U/Pb dates are between 1210 and 1254 Ma, which suggests the Sharbot Lake domain did not experience the younger metamorphism of the Mazinaw domain (Wallach, 1974; Corfu and Easton, 1994). Regional structural patterns in the Sharbot Lake domain are generally domal, reflecting the dominance of plutonic complexes.

3. Robertson Lake shear zone

3.1. Field observations

The RLSZ crops out as a sinuous zone that strikes north-northeast (Figs. 1 and 2). Mylonitic foliation strikes north-northeast, slightly oblique to the regional gneissosity (Figs. 2b and 3). Lineations on mylonite shear planes plunge ~30° to the southeast (Fig. 3b). The RLSZ is 0.5–1.0 km thick, with the cataclastic portion half the thickness of the mylonitic portion (Fig. 4). Detailed traverses indicate that regional foliation and lineation geometries are subparallel to the shear zone within several kilometers of the zone (Fig. 4). East-northeast trending folds of the Mazinaw domain and margins of plutonic complexes adjacent to the zone

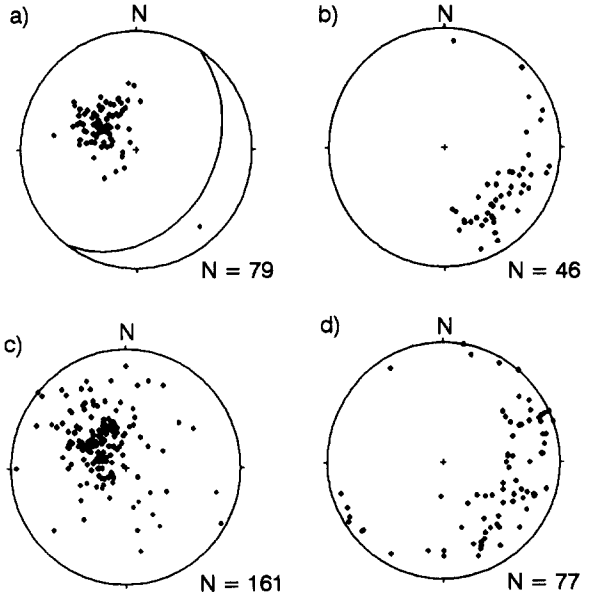

Fig. 3. Equal area lower-hemisphere projections of: (a) poles to mylonitic foliation with great circle of the mean mylonite foliation orientation (N35E, 31SE); (b) mylonitic lineation; (c) poles to regional gneissosity; and (d) regional lineation.

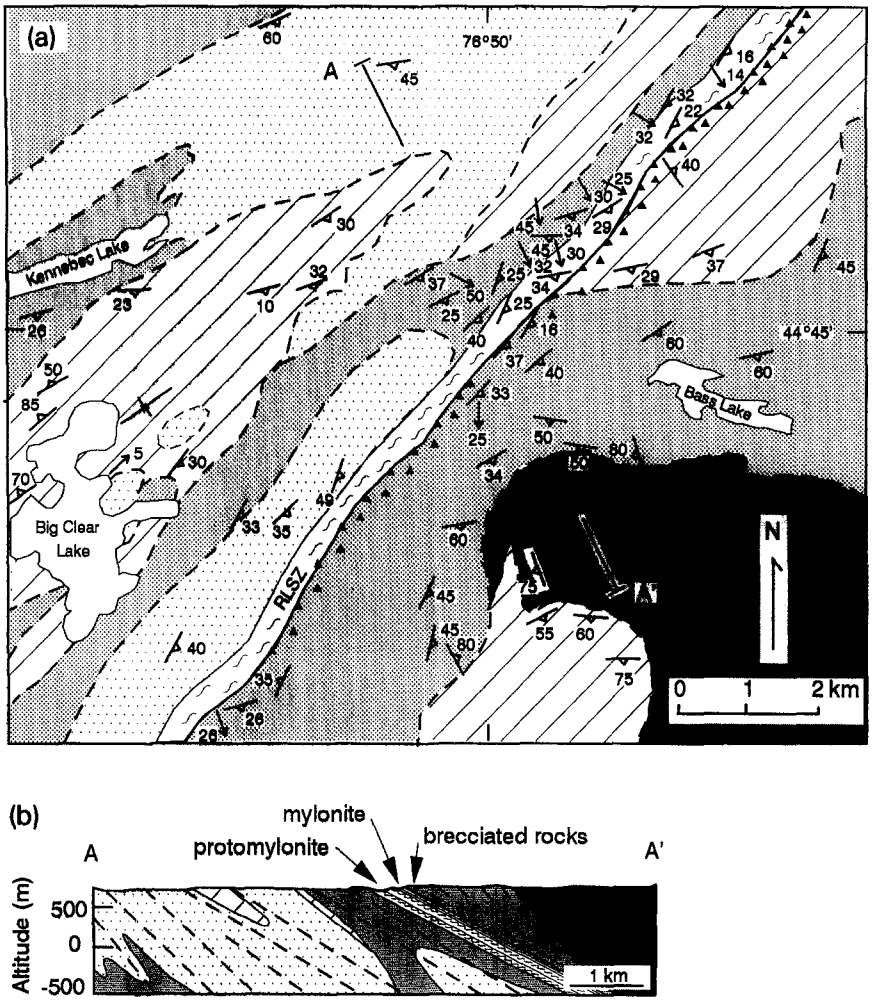

Fig. 4. (a) Detailed geologic map and (b) cross-sections along line *A–A'* illustrating the subparallel regional foliation within several kilometers of the RLSZ and relative thickness of the mylonitic and cataclastic portions of the zone. Rock types are shaded as in Fig. 2a.

are truncated by the RLSZ (Fig. 2). Several thrust shear zones mapped in the Mazinaw domain are truncated by or merge with the RLSZ, although detailed field relations are ambiguous due to lack of exposure (Fig. 1). Along with the contrast in lithology across the zone, this suggests that the RLSZ may be a site of previous thrusting or suturing between the Mazinaw and Sharbot Lake domains. However, field or microstructural evidence for an earlier thrusting history along the RLSZ has not been found. Rock types within the zone are as varied as the regional lithology, but felsic orthogneiss, amphibole schist and marble are the most common rock types.

Granitic mylonites contain lensoidal and sigmoidal porphyroclasts of feldspar surrounded by elongate quartz grains and micaceous folia (Fig. 5a). Quartz grains are generally elongate parallel or oblique to the foliation. The sense of obliquity of elongate grains and micaceous folia is inclined to the west relative to the dominant, east-southeast dipping mylonitic foliation. This composite fabric is a mesoscopic S–C fabric defining a normal (east side down) shear-sense (Berthe et al., 1979; Lister and Snoke, 1980). The finest-grained (~ 10 μm) felsic ultramylonites lack a strong lineation but have a well developed foliation defined by fine compositional lamellae of flattened quartz rods and micaceous interlayers (Fig. 5b).

Amphibole mylonites have lineations defined by alignment of elongate amphibole grains. Anastomosing lamellae composed of fine (< 50 μm in length) amphi-

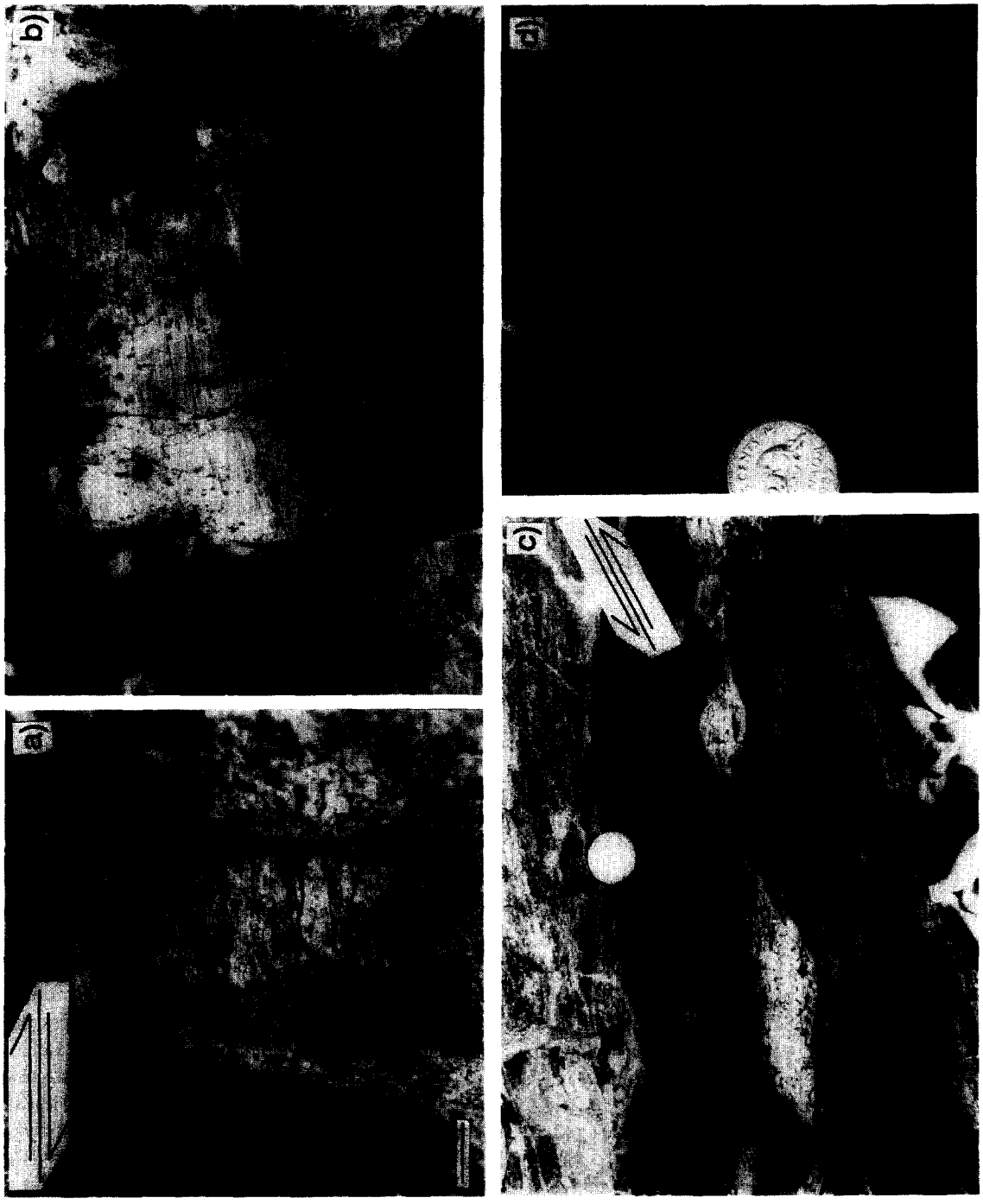

Fig. 5. Field photographs of: (a) protomylonitic granite showing lenticular and sigmoidal feldspar porphyroclasts and quartz ribbons (view of XZ plane, looking north-northeast, scale bar is 1 cm); (b) *ultramylonitic granite showing fine lamellar foliation*; (c) mylonitic amphibolite with displaced, asymmetric felsic pods indicating a sinistral shear-sense (view looking south); and (d) marble mylonite with calc-silicate porphyroclast showing compositional and color lamination.

bole or quartz and plagioclase are commonly deflected around coarser-grained quartzofeldspathic pods that are aligned parallel or oblique to the foliation. Sigmoidal felsic pods in amphibolites are commonly displaced in a normal sense along shear bands (Fig. 5c). Toward the eastern and central portions of the shear zone amphibolites tend to be lighter green in color (reflecting chlorite alteration) and contain abundant veins and fractures compared to black, crystalloblastic amphibole schists away from the shear zone.

Light-colored, coarse-grained marble with coarse graphite flakes becomes fine-grained and dark gray in the mylonite zone reflecting grain size reduction and dissemination of graphite throughout the rock during mylonitization (Fig. 5d). Mylonitic foliation is defined by color and compositional bands of silicate-rich marble. Lineations are defined by graphite streaks and elongate calcite grains in the shear plane. Marble mylonites typically contain large calcite and calc-silicate porphyroclasts that deflect the mylonitic foliation. Porphyroclasts commonly have a sigmoidal geometry and calc-silicate aggregates contain asymmetric tails that merge with the mylonitic foliation. Porphyroclast asymmetries observed in the field also yield a consistent normal shear-sense.

3.2. Mylonite microstructural observations and shear-sense indicators

Thin-sections cut parallel to lineation and perpendicular to foliation were prepared to characterize mylonites in terms of mode and mechanisms of deformation, and to determine shear-sense. Normal (top-down-to-the-east) shear-sense was determined from field and microscopic observations at several locations along the RLSZ (Fig. 2b). Mylonitic granites with S–C textures consistently yield a normal (east side down) sense of shear (Fig. 6a). Oblique mica and quartz ribbon orientations define S-surfaces within domains bounded by shear (C) planes. Shear planes are characterized by truncation of oblique fabric elements, quartz ribbons and fine-grained micaceous lamellae. Granitic mylonites contain evidence for crystal-plastic and brittle deformation mechanisms. Deformation microstructures of feldspar grains are dominated by fractures indicating a component of cataclastic flow. Undulatory extinction, mechanical twins and core–mantle structures are present locally. Quartz ribbons with undulose extinction and subgrain development are ubiquitous. Recrystallized grains within polycrystalline quartz ribbons generally have an oblique shape preferred orientation (Fig. 6b). This shape fabric is analogous to that described in quartzites by Law et al. (1984) and Burg (1986) and yields a shear-sense consistent with the S–C fabrics. Fine-grained granitic ultramylonite samples contain C–C′ composite fabrics that indicate a normal shear-sense (Fig. 6c) (Platt and Vissers, 1980; Malavieille, 1987).

Amphibole mylonites are characterized by very fine grain sizes ($< 50\ \mu m$) and an anastomosing to planar foliation. Amphiboles generally have sharp to slightly patchy extinction. Quartz grains commonly show undulose extinction and subgrain development. Sigmoidal shapes defined by deflected foliation planes near porphyroclasts indicate a normal shear-sense in amphibole mylonite samples.

Microstructurally, calcite mylonites are characterized by large calcite porphyroclasts and a matrix of smaller, equant, dynamically recrystallized grains. Porphyroclasts are commonly twinned and have subgrains (C in Fig. 6d). Equant to slightly elongate matrix grains are mantled by fine secondary phases and have little subgrain development. Phlogopite grains in marble mylonites are commonly kinked and separated along cleavage planes. These micas are aligned parallel or slightly oblique to the mylonitic foliation. The obliquity of mica grains ('mica fish') is similar to that of asymmetric porphyroclasts and also yields a normal shear-sense (M in Fig. 6d).

3.3. Brittle deformation

In addition to the mylonitic microstructures attributed to crystal-plasticity, evidence of brittle deformation is present in a 0.2–0.5 km thick zone overlying mylonites (Fig. 4). Brittle deformation is most intense adjacent to mylonites and decreases in intensity into the hanging wall (Sharbot Lake domain). Using the terminology of Sibson (1977) the fault rocks range from crush breccia with meter-scale clasts to ultracataclasite. Veins containing calcite, epidote, quartz and pyrite are common. The most intensely brecciated rocks are completely altered to chlorite and fine white mica. Ultracataclastic seams occur in zones one millemeter to a few centimeters wide. Less intensely brecciated rocks (crush breccia) contain well defined

Fig. 6. Photomicrographs of shear-sense indicators. (a) S–C–C′ composite texture in granite mylonite showing fractured feldspar (*F*) and oblique quartz ribbon (*Q*). (b) Quartz shape fabric oblique to the shear plane (*C*) in polycrystalline quartz ribbons developed in mylonitic pegmatite. (c) C–C′ Texture in granitic ultramylonite. (d) Mica fish (*M*) in fine-grained marble mylonite with few calcite porphyroclasts (*C*). All photos are taken from thin-sections cut parallel to the mylonitic lineation and perpendicular to the mylonitic foliation (XZ plane).

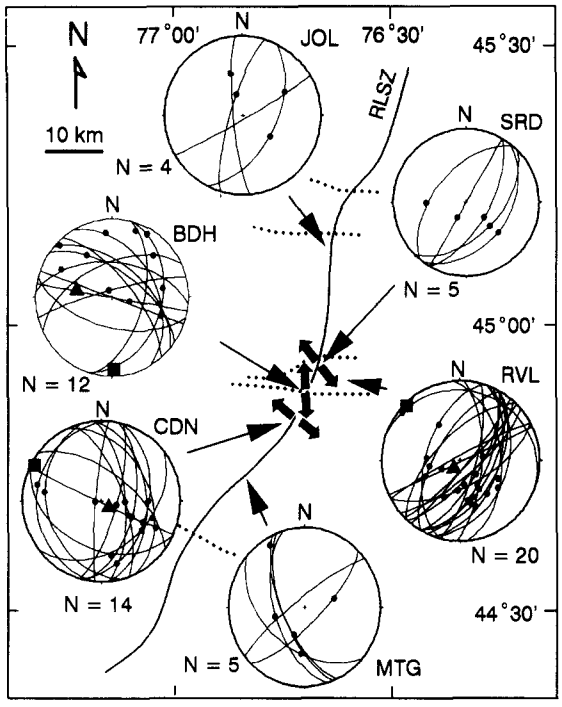

Fig. 7. Equal-area, lower-hemisphere projections of slickensides (great circles) and slickenlines (dots) associated with brittle deformation along the RLSZ. Dotted lines are Paleozoic faults. Solid triangles are σ_1 directions and solid squares are σ_3 directions based on fault inversion analyses. Thick arrows on the map are azimuths of extension directions.

slickensides, which are developed within thin gouge zones. Locally, epidote, quartz and calcite overgrowths on slickensides have a fibrous, stepped habit which allow the sense of slip of the last movement on the surface to be inferred (Petit, 1987). Slickenside and slickenline orientations were measured at several localities along the RLSZ (Fig. 7). Slickensides with down-dip slickenlines generally strike north-northeast and dip steeply east. Slip-sense indicators are dominantly normal.

Paleostress orientations were estimated using the computer program of Sperner et al. (1993) based on the method of Angelier (1989). Given the fault orientations, the method minimizes differences between calculated and measured striation orientations by iteratively changing principal stress directions and stress ratio, $R\ [=(\sigma_2-\sigma_3)/(\sigma_1-\sigma_3)]$. The average angle between measured striation orientations and maximum shear stress calculated for the fault planes (F) and the number of faults with displacement sense contrary to that predicted (nev) are also reported (Table 1). Stations with few fault slip-sense data (<10) were considered less reliable. Southeast–northwest extension directions were obtained using data from two stations (RVL and CDN), which reflects brittle deformation along the RLSZ (Fig. 7, Table 1). The third data set (station BDH), located at the intersection of the RLSZ and a previously mapped fault that strikes east–west, indicates north–south extension. Faults in the region with an east–west orientation are associated with the Paleozoic (post-Middle Ordovician) Ottawa graben (Kumarapeli, 1985) (Fig. 1). These faults are generally high-angle normal faults along which the northern block has moved down, which is consistent with paleostress analysis at this locality.

3.4. Timing of displacement

Plutonic bodies, large-scale regional folds and metamorphic units are cross-cut by the RLSZ. The young-

Table 1
Principal stress orientations from inverse analyses

	Station RVL		Station BDH		Station CDN		Station JOL [a]		Station SRD [a]		Station MTG [a]	
	trend	plunge	trend	plunge	trend	plunge	trend	plunge	trend	plunge	trend	plunge
σ_1	209	79	284	55	127	82	121	2	160	60	315	16
σ_2	48	10	80	32	32	1	31	3	28	21	55	30
σ_3	317	3	177	12	302	8	242	86	290	20	200	55
R	0.247		0.729		0.196		0.757		0.139		0.824	
F	8		15		12		0		2		4	
nev	2		0		0		0		0		1	

[a] Considered unreliable due to paucity of data.

est of these cross-cut units in the footwall contains metamorphic zircons that have crystallization ages between 995 and 1050 Ma (Corfu and Easton, 1995), requiring that the RLSZ was active after 995 Ma. Additionally, the crystal-plastic to brittle nature of the zone indicates activity below temperatures associated with the brittle to plastic transition of quartzofeldspathic rocks (250–350°C; e.g., Sibson, 1983). Thus, a displacement history late in the evolution of the Grenville orogen is inferred from cross-cutting relations and structural observations.

Hornblende $^{40}Ar/^{39}Ar$ cooling ages of 934 ± 3 and 1007 ± 3 Ma obtained by Cosca et al. (1991, 1992) on either side of the zone place the time of shearing at or after ~930 Ma. To further constrain the timing of movement along the RLSZ new $^{40}Ar/^{39}Ar$ data were collected (Table 2). A laser step-heating technique was used on biotite from amphibolite and mica schist. Rock samples were crushed, sieved and biotite grains were selected using a binocular microscope. Grains were cleaned in de-ionized water in an ultrasonic bath. Samples (1–3 grains) were packaged and irradiated at the University of Michigan's Ford Phoenix reactor at location L67 for 90 MWh. Neutron flux gradients were monitored with the MMhb-1 standard using an age of 520.4 Ma (Samson and Alexander, 1984). An argon-ion laser system was used for step-heating by defocusing the beam to uniformly heat the grain(s) and increasing the laser power. Each step consisted of heating for 60 s followed by 2 min of gas purification using two 10 l/s SAES getters (ST101 alloy) and a liquid N_2 cold finger. Argon isotopic ratios (^{40}Ar–^{36}Ar) were measured with a Mass Analyzer Products 215 mass spectrometer with a Nier source and Balzers electron multiplier. Source plus multiplier mass discrimination was determined after each step-heating run by measuring the $^{40}Ar/^{36}Ar$ ratio of 3×10^{-9} cm^3 (STP) of atmospheric argon. Extraction line blanks were measured every five steps. Maximum line blanks measured during the runs were 3×10^{-16} mol for ^{40}Ar, and 2×10^{-18} to 5×10^{-18} mol for ^{39}Ar, ^{38}Ar, ^{37}Ar, and ^{36}Ar. Plateau ages were calculated as the inverse variance weighted mean of dates from steps in the plateau. Criteria used to define a plateau are that the plateau include 50% or more of the total ^{39}Ar released in three or more consecutive steps and the ages of all steps overlap at 2σ. A replicate of each sample was run to evaluate reproducibility and grain to grain variability between analyses.

The biotite step-heating spectra obtained have ^{40}Ar loss characteristics for the first few steps (Fig. 8). However, the spectra have consistent ages over most of the ^{39}Ar release, yielding plateaus ages of 901 ± 1 and 986 ± 1 Ma on either side of the shear zone (Figs. 2a, 8). Sample LVT130B has a plateau age identical to the total gas age. Therefore, this sample is inferred to have cooled through the biotite closure temperature at 901 Ma. Sample RVL118B has a spectrum indicative of significant ^{40}Ar loss and disparate total gas and plateau ages. Although this loss may be due to an episodic thermal event, there is no information to support this interpretation. The spectra is interpreted to have undergone diffusive loss of ^{40}Ar during slow cooling and the cooling age is inferred from the total gas age (969 Ma).

The closure temperature (T_c) for Ar in biotite (~300°C) is lower than that of hornblende (~500°C) (Dodson, 1979; Harrison, 1981; Harrison et al., 1985; Grove and Harrison, 1993). If biotite cooling ages were similar on either side of the zone, activity must have ceased prior to the time at which the region passed through the biotite closure temperature. On the other hand, shear zone activity contemporaneous with or post-cooling (through T_c) would result in offset cooling ages, thereby signifying continued shear zone activity at least until the cooling age in the footwall rocks. The closure temperature of biotite may depend on composition, although the details of this dependence are ambiguous (Harrison et al., 1985; Grove and Harrison, 1993). Biotites analyzed have similar compositions (41% versus 51% annite, Table 3) so the difference in closure temperature associated with this minor compositional difference cannot account for the 68 m.y. difference in cooling age between the biotites. The difference in biotite cooling ages on either side of the shear zone is attributed to displacement across the zone that occurred until at least 901 Ma and possibly later. The temperature (300°C) of the footwall rocks at 901 Ma is consistent with the transition from crystal-plastic to brittle deformation that is inferred from field observations.

4. Discussion

Extensional deformation in the Grenville orogen has only recently been recognized (Hanmer, 1988; Carlson

Table 2
Argon isotope data obtained during biotite step-heating runs

1 Power (mW)	2 ^{39}Ar fraction of total	3 $^{39}Ar_K$ moles	4 $^{40}Ar/^{39}Ar$	5 $^{38}Ar/^{39}Ar$	6 $^{37}Ar/^{39}Ar$	7 $^{36}Ar/^{39}Ar$	8 $^{40}Ar^*/^{39}Ar_K$	9 % ^{40}Ar atmos.	10 Age (Ma)	11 error (Ma) 1σ
RVL118B Biotite										
100	0.008	8.86E-14	46.704	0.646154	0.985850	0.018907	31.2731	33.0	348	12
200	0.086	9.75E-13	94.712	0.398463	0.255223	0.002006	93.0859	1.7	886	3
240	0.106	1.21E-12	106.772	0.428569	0.252102	0.002290	106.504	0.3	984	3
260	0.142	1.62E-12	107.403	0.216031	0.248529	0.000829	107.010	0.4	988	2
265	0.063	7.15E-13	105.988	0.725161	0.243907	0.002310	105.788	0.2	979	5
280	0.045	5.09E-13	107.021	0.431890	0.247099	0.001903	106.437	0.5	984	4
320	0.077	8.79E-13	106.365	0.520602	0.248728	0.002250	105.989	0.4	981	4
360	0.070	7.99E-13	107.400	0.581182	0.249597	0.002069	107.152	0.2	989	4
400	0.092	1.05E-12	106.987	0.309926	0.250267	0.002235	106.680	0.3	985	2
440	0.051	5.81E-13	106.188	0.421400	0.247790	0.002386	105.673	0.5	978	3
480	0.051	5.77E-13	105.688	0.628307	0.245127	0.003004	105.119	0.5	974	5
520	0.042	4.74E-13	106.044	0.736085	0.250204	0.002483	105.630	0.4	978	6
560	0.040	4.50E-13	104.397	0.565552	0.241852	0.002736	104.057	0.3	967	5
620	0.039	4.42E-13	105.648	0.436610	0.245551	0.002644	105.215	0.4	975	3
700	0.038	4.32E-13	105.947	0.717389	0.254620	0.003160	105.706	0.2	979	5
800	0.016	1.81E-13	106.254	0.721964	0.254987	0.004437	105.273	0.9	975	8
1000	0.021	2.41E-13	105.047	0.737873	0.257478	0.003895	104.096	0.9	967	6
2000	0.015	1.74E-13	104.651	0.594847	0.263292	0.004055	104.591	0.1	971	6
J = 0.006812	±0.000014									
total gas age =	969±2									
plateau age (240-400) =	986±1		mswd 1.0							
LVT130B Biotite										
20	0.000	3.84E-15	66.82	3.744659	0.125992	0.022705	33.9703	49.2	396	120
40	0.001	1.15E-14	88.51	1.670375	0.136638	0.012636	60.9772	31.1	658	34
60	0.013	1.44E-13	88.97	0.468630	0.009477	0.001498	85.0665	4.4	864	5
80	0.015	1.74E-13	90.54	0.462493	0.006123	0.000844	88.9819	1.7	895	4
100	0.015	1.76E-13	88.67	0.397788	0.004859	0.000682	87.1141	1.7	881	4
120	0.037	4.20E-13	89.90	0.309144	0.004214	0.000330	89.0048	1.0	896	3
130	0.019	2.15E-13	90.42	0.207922	0.005507	0.001135	88.4918	2.1	892	2
140	0.044	5.06E-13	89.25	0.302410	0.002918	0.000626	88.6608	0.7	893	3
150	0.014	1.61E-13	90.16	0.427686	0.003631	0.001214	89.2634	1.0	898	4
160	0.024	2.70E-13	90.35	0.258232	0.003278	0.001000	89.5430	0.9	900	2
170	0.050	5.65E-13	90.47	0.291821	0.002835	0.000395	89.7109	0.8	901	2
180	0.044	4.98E-13	90.57	0.395576	0.003019	0.000418	89.6605	1.0	901	3
200	0.047	5.38E-13	90.79	0.322024	0.003364	0.000424	89.3872	1.5	899	3
260	0.046	5.21E-13	90.33	0.318925	0.003763	0.000686	89.1899	1.3	897	3
300	0.089	1.01E-12	90.34	0.227065	0.003042	0.000257	89.7926	0.6	902	2
340	0.036	4.14E-13	90.67	0.220164	0.003818	0.000788	89.6036	1.2	900	2
380	0.086	9.76E-13	90.65	0.208806	0.003147	0.000236	90.1951	0.5	905	2
440	0.068	7.78E-13	90.24	0.227255	0.002914	0.000416	89.8202	0.5	902	2
500	0.167	1.90E-12	90.81	0.129090	0.003181	0.000283	90.5362	0.3	908	1
2000	0.186	2.11E-12	90.38	0.114836	0.002315	0.000181	90.2102	0.2	905	1
J = 0.007222	±0.000007									
total gas age =	901±1									
plateau age (150-440) =	901±1		mswd 1.1							

Columns: 1 = laser power (beam diameter 1.5 mm); 2 = fraction ^{39}Ar released; 3 = moles of K-derived ^{39}Ar in step. 4–7 = isotopic ratios corrected for blank, mass discrimination, Ca-, K-, and Cl-derived Ar isotopic interference, decay of ^{37}Ar, and ^{36}Ar from decay of ^{36}Cl. 8 = ratio of radiogenic ^{40}Ar to K-derived ^{39}Ar. 9 = %^{40}Ar atmospheric of total ^{40}Ar in fraction. 10 = apparent ages calculated using decay constants recommended by Steiger and Jäger (1977). 11 = includes uncertainties in J, mass discrimination, blank, and isotopic measurements.

et al., 1990; Culshaw et al., 1994). In the Metasedimentary Belt, the Bancroft shear zone has been documented as a synorogenic extensional shear zone active from 1045 to 1030 Ma (Mezger et al., 1991), which initiated during compressional tectonics and continued until at least 960 Ma (van der Pluijm et al., 1994). Based on the geochronologic data presented here extension along the RLSZ was active until at least 901 Ma. Thus, the Metasedimentary Belt has at least a 130 m.y. history of extensional deformation, which occurred later in the southeast Metasedimentary Belt based on brittle structures unique to the RLSZ.

The RLSZ is a low-angle (~ 30°), crystal-plastic to brittle extensional shear zone in the Metasedimentary Belt of the Grenville orogen. Seismic reflectors that dip ~ 13° have been interpreted to correlate with the RLSZ (White et al., 1994; Zelt et al., 1994). In these studies, the RLSZ is a major thrust fault that juxtaposes relatively high acoustic velocity rocks of the hanging wall with less dense rocks of the footwall. However, the field data do not support a thrust shear-sense along the RLSZ. Rather, our results emphasize that the mode of unroofing and exhumation of the Metasedimentary Belt was characterized by extensional faulting. The RLSZ may be a reactivated suture zone or thrust fault, but the present data conclusively support an extensional history only.

The RLSZ is composed of three components: protomylonites, mylonites and breccias that were juxtaposed as the ambient temperature decreased during exhumation of this fault system (e.g. Grocott, 1977; Passchier, 1984). Based on the relative thickness of the cataclastic versus crystal-plastic portions of the shear zone, shallow-level, brittle deformation was more

Table 3
Representative biotite compositions determined by electron microprobe analysis

	LVT130B	RVL118B
Wt% oxid		
SiO_2	36.14	35.75
TiO_2	1.66	2.01
Al_2O_3	19.00	16.15
Cr_2O_3	0.03	0.00
FeO	15.53	20.73
MnO	0.24	0.16
MgO	12.41	11.03
BaO	0.17	0.42
CaO	0.02	0.08
Na_2O	0.29	0.09
K_2O	9.52	9.02
F	0.60	0.16
Cl	0.00	0.34
H_2O	2.81	3.30
O=F	-0.25	-0.07
O=Cl	0.00	-0.08
Total	98.16	99.10
# of ions normalized to 14 cations		
Si	5.529	5.548
Aliv	2.471	2.452
Alvi	0.956	0.502
Ti	0.191	0.235
Cr	0.004	0.000
Fe	1.988	2.690
Mn	0.031	0.021
Mg	2.830	2.552
Ba	0.010	0.026
Ca	0.003	0.014
Na	0.085	0.027
K	1.858	1.785
A site	1.943	1.812
O	20.000	20.000
O (OH site)	0.841	0.412
F	0.290	0.080
Cl	0.000	0.090
OH	2.868	3.418
Mg#	0.587	0.487

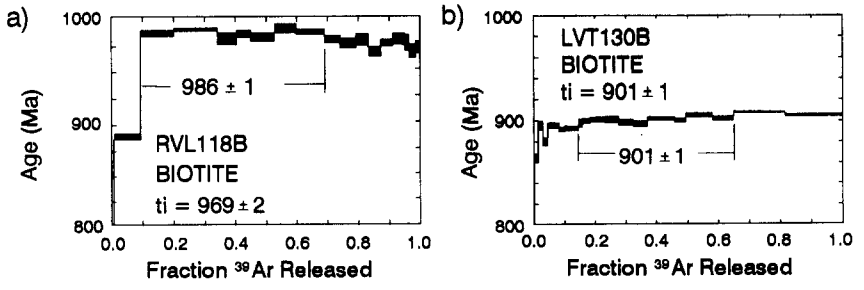

Fig. 8. Ar-release spectra with $\pm 1\sigma$ errors from biotite samples located in (a) the hanging wall and (b) the footwall. Total gas ages are given as t_i. Sample locations are shown in Fig. 2. The spectra indicate ^{40}Ar loss in the first few steps. Displacement prior to cooling through the closure temperature would yield similar ages on either side of the zone. Therefore, these data indicate RLSZ activity at least until 901 Ma. Universal Transverse Mercator grid coordinates are 4971225N, 372600E for sample RVL118B, and 4990750N, 361920E for smaple LVT130B.

localized than the deep-level, plastic deformation (Fig. 4). Sibson (1977) presented a conceptual model for fault zones that predicted narrowing and increased localization of fault displacement over the transition from 'quasi-plastic' to 'elastico-frictional' deformation processes. Bak et al. (1975) described a well exposed example of a shear zone in Greenland with width decreasing and shear strain increasing toward shallower structural levels. The structural observations of the plastic to brittle RLSZ are in accord with these studies.

The Mohr–Coulomb criterion and Andersonian fault models predict normal fault dips of ~60° (Anderson, 1951). However, in many extensional terranes low-angle (<30°) normal faults have been described, which do not follow the Andersonian fault model (e.g. McKenzie, 1978; Coney, 1980; Shackelford, 1980; Scott and Lister, 1992). Scott and Lister (1992) argued for a low-angle origin for normal faulting in a metamorphic core complex in the Basin and Range province. A general mechanical model for low-angle normal faulting in isotropic crust has not been developed, but several hypotheses have been developed to explain initiation of low-angle normal faults. The circumstances required in these models are varied: (a) synextensional magmatism alters the stress field thereby mechanically favoring low-angle geometries (Parsons and Thompson, 1993); (b) major crustal flexure alters the stress field (Spencer and Chase, 1989); and (c) pre-existing interfaces or structural weakness guides otherwise mechanically unfavorable fault geometries (Davis and Coney, 1979; Brun and Choukroune, 1983). An alternative explanation for low-angle normal faults is rotation of relatively high-angle (60°) faults to low-angles (30° dip) during extension (e.g. Davis, 1983).

Initiation of low-angle normal faulting along the RLSZ cannot be related to synextensional magmatism. At a few localities, pegmatitic pods occur within the RLSZ but these are not obviously synextensional. In addition, the igneous rocks deformed in the RLSZ are intensely deformed during crystal-plastic deformation of old (>1200 Ma) protoliths (e.g. van Breeman and Davidson, 1988; Corfu and Easton, 1994). The most recent magmatism is high-K_2O magmatism that occurred between 1089 and 1076 Ma (Corriveau and Gorton, 1993). These rocks are not spatially correlative with the RLSZ and predate extension in the region (Mezger et al., 1991). Flexure of the crust in response to crustal loading during or following shortening cannot be evaluated using presently available data because the Grenville orogen is an ancient mountain belt. The model of Spencer and Chase (1989) may be testable and applicable to the Basin and Range province in the western U.S., but its application to the Grenville is ambiguous. A pre-existing interface, and contrasting lithologies, are present along the RLSZ. The Sharbot Lake domain is dominated by large mafic plutonic complexes while the Mazinaw domain is composed of metasedimentary, metavolcanic, and felsic gneisses (Fig. 2a). Other zones of weakness may be thrust faults mapped near the RLSZ. However, these are oblique to the zone and no field evidence exists for previous thrusting along the RLSZ. As discussed below, structural weakness may have played a role in the development of the RLSZ based on the contrast in lithology (possible suture site) and ubiquitous brecciated rocks adjacent to mylonites.

Assuming that the metamorphic isograds were horizontal before extension, the west to east increase in metamorphic grade in the hanging wall and footwall indicates that rotation accompanied displacement during the transition from plastic to brittle processes. Using the modes of extension outlined by Wernicke and Burchfiel (1982), block rotations are associated with planar or listric faults. Rotations associated with a planar fault require rotation of the fault along with rotation of the blocks (domino block fault model; Davidson, 1989). The domino block fault model is unlikely considering the spacing of known extensional faults in the Metasedimentary Belt and thus the size of rotating blocks: the Bancroft shear zone is ~80 km west of the RLSZ (Fig. 1). Given that amphibolite-facies rocks occur in the footwall adjacent to the RLSZ, a minor rotation of say 10° would require lower greenschist to sub-greenschist rocks in the hanging wall adjacent to the Bancroft shear zone. Such low-grade metamorphic rocks are not observed.

Mylonitic shear foliations dip 30° east-southeast while brittle fault surfaces dip 60° east-southeast, cutting mylonitic foliations. The discrete brittle faults occur along a cataclastic zone parallel to the mylonite zone. A listric fault may produce structures consistent with those observed. However, displacement will only produce rotation in the hanging wall and not account for the observed west to east increase in metamorphic grade in the footwall. Wernicke and Axen (1988)

describe the evolution of listric fault systems accompanied by isostatic uplift of the footwall, which may produce such a difference in metamorphic grade. They depict sequential slicing of the hanging wall to maintain the listric geometry as displacement occurs. However, different field relations are observed along the RLSZ. The cataclastic portion of the shear zone always occurs adjacent to and within the mylonite zone. This observation suggests that brittle deformation was localized along the mylonite zone. If sequential slicing of the hanging wall occurred, brittle faults should be observed cutting the hanging wall, but they are not. The listric model then requires that the observation that mylonites always occurring adjacent to breccias is coincidental (i.e. the erosional level is consistently at the intersection of the brittle faults and mylonite zone).

Based on the arguments above, a model describing the evolution of the RLSZ must involve distortion of the hanging wall and footwall and maintain the location of the shear zone through the transition from plastic to brittle processes. A geometric model consistent with these observations is outlined in Fig. 9. Initiation of the shear zone follows the Mohr–Coulomb criterion and Andersonian faulting (Fig. 9a). Subsequent displacement unloads the footwall, and footwall uplift and flexural rotations occur (Buck, 1988), which reduce the dip of the shear zone. Continued displacement further shallows the shear zone and juxtaposes mylonites and breccia (Figs. 9b, 9c). Brittle deformation is accommodated along discrete high-angle faults within the breccia zone, which follows the structurally weak zone produced by mylonitization (Fig. 9c). The geometric observations and metamorphic data thus require a model of shear localization along a previously weakened zone and rotation due to isostatic flexural rotations of the footwall and hanging wall.

The observations and model given here may be applicable to regions which have likely undergone greater magnitudes or more widespread extension, such as the Basin and Range province of southwestern North America. Detachment faults that bound metamorphic core complexes are associated with tens of kilometers of extension and typically have dips of $<25°$ (e.g. Wernicke, 1981; Davis, 1987). These faults generally underlie hanging walls with domino and listric fault arrays and fault blocks. Perhaps a critical dip angle ($\sim 25°$) is reached during rotation of extensional faults before new faults dissect the hanging wall (Jackson, 1987; Jackson et al., 1988). Thus, the RLSZ may represent a deep-seated, early stage equivalent of normal faulting in regional extensional terranes such as the Basin and Range province.

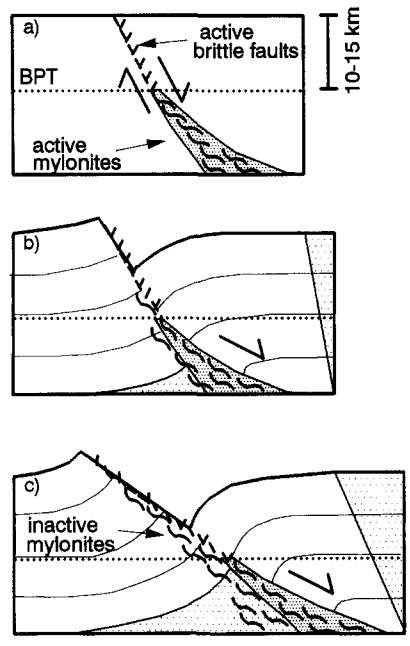

Fig. 9. Geometric model of extension associated with the RLSZ consistent with the observed differences in metamorphic grade and shear zone geometry. (a) Initial high-angle (60°) shear zone widening and possibly shallowing with depth. *BPT* is the transition from brittle to crystal-plastic dominated deformation processes. Dark stipple is active mylonite. Small ticks are discrete brittle faults. (b) Subsequent displacement initiates flexural rotations in the footwall and hanging wall and juxtaposes mylonite and breccia. Thin lines schematically represent isograds. Light stipple indicates area added to the section. (c) Cataclastic deformation is accommodated along discrete high-angle faults (small ticks) in the breccia zone that has rotated to a low angle (30°). The breccia zone is localized along the previously weakened mylonite zone. Subsequent erosion leads to west to east increase metamorphic grades in the hanging wall and footwall, and offset metamorphic grade across the zone.

Acknowledgements

Grants from the National Science Foundation (EAR 91-19196 and EAR 93-05736), the Scott Turner Fund (at the University of Michigan), and Geological Society of America (4875-92 and 5122-93) provided financial support for this project. R.M. Easton first introduced us to the RLSZ and his field assistance and

insights into the regional geology were critical for work presented here. We are grateful for field assistance and access to the field area provided by Roy Ferguson (Snow Road), Carson Lewis (Mountain Grove), Ray Taylor (Sheffield Lake) and many other friendly people of Ontario, Canada. E. Essene, J. Magloughlin, C. Onasch, S. Richard, and M. Steltenpohl are thanked for reviewing earlier versions of this paper. Chris Hall, Alex Halliday, and Marcus Johnson are thanked for training and assistance in $^{40}Ar/^{39}Ar$ analyses at the Radiogenic Isotope Geochemistry Laboratory at the University of Michigan. David van Everdinger and Jeroen van Gool provided graphics software (QUICKPLOT) for orientation data. M.A. Cosca, G.H. Davis, C.W. Passchier (journal referees) are thanked for their comments and suggestions which helped to improve the paper.

References

Anderson, E.M., 1951. The Dynamics of Faulting (2nd ed.). Oliver and Boyd, Edinburgh, 206 pp.

Angelier, J., 1989. From orientation to magnitudes in paleostress determinations using fault slip data. J. Struct. Geol., 11: 37–50.

Bak, J., Korstgard, J. and Sorensen, K., 1975. A major shear zone within the Nagssugtoqidian of west Greenland. Tectonophysics, 27: 191–209.

Bell, K. and Blenkinsop, J., 1980. Rubidium–strontium isotope studies in the Grenville Province of southeast Ontario. In: Current Research, Part B, Geol. Surv. Can. Pap., 79-1B: 167–170.

Berthe, D., Chroukroune, P. and Jegouzo, P., 1979. Orthogneiss, mylonite and non coaxial deformation of granites: the example of the South Armorican Shear Zone. J. Struct. Geol., 1: 31–42.

Brun, J.-P. and Choukroune, P., 1983. Normal faulting, block tilting, and decollement in a stretched crust. Tectonics, 2: 345–356.

Buck, W.R., 1988. Flexural rotation of normal faults. Tectonics, 7: 959–973.

Burg, J.P., 1986. Quartz shape fabric variations and c-axis fabrics in a ribbon-mylonite: arguments for an oscillating foliation. J. Struct. Geol., 8: 123–131.

Carlson, K.A., van der Pluijm, B.A. and Hanmer, S., 1990. Marble mylonites of the Bancroft shear zone: evidence for extension in the Canadian Grenville. Geol. Soc. Am. Bull., 102: 174–181.

Carmichael, D.M., Moore, J.M. and Skippen, G.B., 1978. Isograds around the Hastings Metamorphic 'Low'. Geol. Soc. Am.—Geol. Assoc. Can.—Mineral. Assoc. Can., Toronto 1978, Field Trip Guidebook, pp. 325–346.

Carter, T.R., 1981. Copper–Antimony–Gold–Silver Deposits of the Lavant–Darling Area, Southeastern Ontario: Geology, Genesis and Metallogenic Significance. M.Sc. thesis, University of Toronto, Toronto, Ont., 203 pp.

Coney, P.J., 1980. Cordilleran metamorphic core complexes: an overview. Geol. Soc. Am. Mem., 153: 7–31.

Corfu, F. and Easton, R.M., 1994. U/Pb geochronology of the Mazinaw terrane, Central Metasedimentary Belt, Grenville Province, Ontario. Prog. Abstr., Geol. Assoc. Can.—Mineral. Assoc. Can., A22, 19 pp. .

Corfu, F. and Easton, R.M., 1995. U/Pb geochronology of the Mazinaw terrane, an imbricate segment of the Central Metasedimentary Belt, Grenville Province, Ontario. Can. J. Earth Sci., in press.

Corriveau, L. and Gorton, M.P., 1993. Coexisting K-rich alkaline and shoshinitic magmatism of the arc affinities in the Proterozoic: a reassessment of syenitic stocks in the southwestern Grenville Province. Contrib. Mineral. Petrol., 113: 262–279.

Cosca, M.A., Sutter, J.F. and Essene, E.J., 1991. Cooling and inferred uplift/erosion history of the Grenville Orogen, Ontario: constraints from $^{40}Ar/^{39}Ar$ thermochronology. Tectonics, 10: 959–977.

Cosca, M.A., Essene, E.J., Kunk, M.J. and Sutter, J.F., 1992. Differential unroofing within the Central Metasedimentary Belt of the Grenville Orogen: constraints from $^{40}Ar/^{39}Ar$ thermochronology. Contrib. Mineral. Petrol., 110: 211–225.

Culshaw, N.G., Ketchum, J.W.F., Wodicka, N. and Wallace, P., 1994. Deep crustal ductile extension following thrusting in the southwestern Grenville Province, Ontario. Can. J. Earth Sci., 31: 160–175.

Davidson, A., 1984. Tectonic boundaries within the Grenville Province of the Canadian shield. J. Geodyn., 1: 433–444.

Davidson, I., 1989. Extensional domino fault tectonics: kinematics and geometrical constraints. Ann. Tectonicae, III: 12–24.

Davis, G.H., 1983. Shear-zone model for the origin of metamorphic core complexes. Geology, 11: 342–347.

Davis, G.H., 1987. A shear-zone model for the structural evolution of metamorphic core complexes in southeastern Arizona. In: M.P. Coward, J.F. Dewey and P.L. Hancock (Editors), Continental Extensional Tectonics. Geol. Soc. London, Spec. Publ., 28: 247–266.

Davis, G.H. and Coney, P.J., 1979. Geologic development of the Cordilleran metamorphic core complexes. Geology, 7: 120–124.

Dodson, M.H., 1979. Theory of cooling ages. In: E. Jager and J.C Hunziker (Editors), Lectures in Isotope Geology. Springer-Verlag, Berlin, pp. 195–202.

Easton, R.M., 1986. Geochronology of the Grenville Province. In: J.M. Moore, A. Davidson and A.J. Baer (Editors), The Grenville Province. Geol. Assoc. Can. Spec. Pap., 31: 127–173.

Easton, R.M., 1988a. Geology of the Darling area Lanark and Renfrew counties. Ont. Geol. Surv. Open File Rep., 5693, 206 pp.

Easton, R.M., 1988b. Regional mapping and stratigraphic studies, Grenville Province with some notes on mineralization environments. In: A.C. Colvine, M.E. Cherry, B.O. Dressler, P.C. Thruston, C.L. Baker, R.B. Barlow and C. Riddle (Editors), Summary of Field Work and Other Activities. Ont. Geol. Surv. Misc. Pap., 141: 300–308.

Easton, R.M., 1988c. The Robertson Lake mylonite zone—A major tectonic boundary in the Central Metasedimentary Belt, eastern Ontario. Prog. Abstr., Geol. Assoc. Can.—Mineral. Assoc. Can.—Can. Soc. Pet. Geol. Joint Meeting, 13: A34–A35.

Easton, R.M., 1992. The Grenville Province and the Proterozoic history of central and southern Ontario, Part 2. In: P.C. Thurston, H.R. Williams, R.H. Sutcliffe and G.M. Stott (Editors), Geology of Ontario. Ont. Geol. Surv. Spec. Vol., 4: 714–904.

Ford, F., 1992. Geology of the Fernleigh and Ompah 'synclines', Palmerston Lake area. Ont. Geol. Surv. Misc. Pap., 160: 41–46.

Grocott, J., 1977. The relationship between Precambrian shear belts and modern fault systems. J. Geol. Soc. London, 133: 257–262.

Grove, M. and Harrison, T.M., 1993. Compositional controls governing Argon loss in biotite. Eos Trans. Am. Geophys. Union, 74: 339.

Hanmer, S., 1988. Ductile thrusting at mid-crustal levels, southwestern Grenville Province. Can. J. Earth Sci., 25: 1049–1059.

Harrison, T.M., 1981. Diffusion of ^{40}Ar in hornblende. Contrib. Mineral. Petrol., 78: 324–331.

Harrison, T.M., Duncan, I. and McDougall, I., 1985. Diffusion of 40Ar in biotite: Temperature, pressure and compositional effects. Geochim. Cosmochim. Acta, 49: 2461–2468.

Hutcheon, I. and Moore, J.M., 1973. The Tremolite isograd near Marble lake, Ontario. Can. J. Earth Sci., 10: 936–947.

Jackson, J.A., 1987. Active normal faulting and crustal extension. In: M.P. Coward, J.F. Dewey and P.L. Hancock (Editors), Continental Extensional Tectonics. Geol. Soc. Spec. Publ., 28: 3–17.

Jackson, J.A., White, N.J., Garfunkel, Z. and Anderson, H., 1988. Relations between normal-fault geometry, tilting and vertical motions in extensional terrains: an example from the southern Gulf of Suez. J. Struct. Geol., 10: 155–170.

Jackson, V.A., 1980. Geologic Setting of Mylonitic Rocks in the White Mountain Area, Grenville Province, Southeastern Ontario. B.Sc. Thesis, Carlton University, Ottawa, Ont., 65 pp.

Kumarapeli, P.S., 1985. Vestiges of lapetan rifting in the craton west of the northern Appalachians. Geosci. Can., 12: 54–59.

Law, R.D., Knipe, R.J. and Dayan, H., 1984. Strain path partitioning within thrust sheets: microstructural and petrofabric evidence from the Moine Thrust zone at Loch Eriboll, northwest Scotland. J. Struct. Geol., 6: 477–497.

Lister, G.S. and Snoke, A.W., 1980. S–C Mylonites. J. Struct. Geol., 6: 617–638.

Lumbers, S.B., Heaman, L.M., Vertolli, V.M. and Wu, T., 1990. Nature and timing of Middle Proterozoic magmatism in the Central Metasedimentary Belt, Grenville Province, Ontario. In: C.R. Gower, T. Rivers and A.B. Ryan (Editors), Mid-Proterozoic Laurentia–Baltica. Geol. Assoc. Can. Spec. Pap., 38: 243–278.

Malavieille, J., 1987. Kinematics of compressional and extensional ductile shearing deformation in a metamorphic core complex of the northeastern Basin and Range. J. Struct. Geol., 9: 541–554.

McEachern, S.J. and van Breemen, O., 1993. Age of deformation within the Central Metasedimentary Belt boundary thrust zone, southwest Grenville Orogen: constraints on the collision of the Mid-Proterozoic Elzevir terrane. Can. J. Earth Sci., 30: 1155–1165.

McKenzie, D., 1978, Active tectonics of the Alpine–Himalayan belt: the Aegean Sea and surrounding regions. Geophys. J. R. Astron. Soc., 55: 217–254.

Mezger, K., van der Pluijm, B.A., Essene, E.J. and Halliday, A.N., 1991. Synorogenic collapse: a perspective from the middle crust, the Proterozoic Grenville Orogen. Science, 254: 695–698.

Mezger, K., Essene, E.J., van der Pluijm, B.A. and Halliday, A.N., 1993. U–Pb geochronology of the Grenville Orogen of Ontario and New York: constraints on ancient crustal tectonics. Contrib. Mineral. Petrol., 114: 13–26.

Moore, J.M., Jr. and Thompson, P.H., 1980. The Flinton Group: a late Precambrian metasedimentary succession in the Grenville Province of eastern Ontario. Can. J. Earth Sci., 17: 1685–1707.

Ontario Geological Survey, 1992a. Bedrock geology of Ontario, southern sheet, map 2544, scale 1:1,000,000.

Ontario Geological Survey, 1992b. Tectonic assemblages of Ontario, southern sheet, map 2578, scale 1:1,000,000.

Parsons, T. and Thompson, G.A., 1993. Does magmatism influence low-angle normal faulting. Geology, 21: 247–250.

Passchier, C.W., 1984. Mylonite-dominated footwall geometry in a shear zone, central Pyrenees. Geol. Mag., 121: 429–436.

Pauk, L., 1989a. Geology of the Lavant area, Lanark and Frontenac Counties. Ont. Geol. Surv. Rep., 253, 61 pp.

Pauk, L., 1989b. Geology of the Dalhousie Lake area, Lanark and Frontenac Counties. Ont. Geol. Surv. Rep., 245, 57 pp.

Petit, J.P., 1987. Criteria for the sense of movement on fault surfaces in brittle rocks. J. Struct. Geol., 9: 597–608.

Platt, J.P. and Vissers, R.L.M., 1980. Extensional structures in anisotropic rocks. J. Struct. Geol., 2: 397–410.

Rivers, T., Martignole, J., Gower, C.F. and Davidson, A., 1989. New tectonic subdivisions of the Grenville Province, Southeast Canadian Shield. Tectonics, 8: 63–84.

Sager-Kinsman, E.A. and Parrish, R.R., 1993. Geochronology of detrital zircons from the Elzevir and Frontenac terranes, Central Metasedimentary Belt, Grenville Province, Ontario. Can. J. Earth Sci., 30: 465–473.

Samson, S.D. and Alexander, E.C., Jr., 1987. Calibration of the interlaboratory ^{40}Ar–^{39}Ar dating standard, MMhb-1. Chem. Geol., 66: 27–34.

Scott, R.J. and Lister, G.S., 1992. Detachment faults: evidence for low-angle origin. Geology, 20: 833–836.

Sethuraman, K. and Moore, J.M., Jr., 1973. Petrology of metavolcanic rocks in the Bishop Corners–Donaldson Area, Grenville Province, Ontario. Can. J. Earth Sci., 10: 589–614.

Shackelford, T.J., 1980. Tertiary tectonic denudation of a Mesozoic–early Tertiary(?) gneiss complex, Rawhide Mountains, western Arizona. Geology, 8: 190–194.

Sibson, R.H., 1977. Fault rocks and fault mechanisms. J. Geol. Soc. London, 133: 191–213.

Sibson, R.H., 1983. Continental fault structure and the shallow earthquake source. J. Geol. Soc. London, 140: 741–767.

Smith, B.L., 1958. Geology of the Clarendon–Dalhousie area. Ont. Dept. Mines Ann. Rep. 1956, 45: 1–46.

Spencer, J.E. and Chase, C.G., 1989. Role of crustal flexure in initiation of low-angle normal faults and implications for structural evolution of the Basin and Range Province. J. Geophys. Res., 94: 1765–1775.

Sperner, B., Ratschbacher, L. and Ott, R., 1993. Fault-stria analysis: A TURBO PASCAL program package for graphical presentation and reduced stress tensor calculation. Comp. Geosci., 19: 1361–1388.

Steiger, R.H. and Jäger, E., 1977. Subcommission on geochronology: Convention on the use of decay constants in geo- and cosmochronology. Earth Planet. Sci. Lett., 36: 359–362.

Van Breemen, O. and Davidson, A., 1988. U–Pb zircon ages of granites and syenites in the Central Metasedimentary Belt, Grenville Province, Ontario: radiogenic age and isotopic studies, Report 2. Geol. Surv. Can. Pap., 88-2: 45–50.

Van der Pluijm, B.A. and Carlson, K.A., 1989. Extension in the Central Metasedimentary Belt of the Ontario Grenville: timing and tectonic significance. Geology, 17: 161–164.

Van der Pluijm, B.A., Mezger, K., Cosca, M.A. and Essene, E.J., 1994. Determining the significance of high-grade shear zones by using temperature–time paths, with examples from the Grenville orogen. Geology, 22: 743–746.

Wallach, J.L., 1974. Origin of the Hinchinbrook gneiss and its age relationship to Grenville Group rocks of southeastern Ontario. Geol. Assoc. Can. Annual Meeting, 3rd Circular Abstracts, St. Johns Newfoundland, p. 96.

Wernicke, B., 1981. Low angle normal faulting in the Basin and Range Province: nappe tectonics in and extending orogen. Nature, 291: 645–648.

Wernicke, B. and Axen, G.J., 1988. On the role of isostacy in the evolution of normal fault systems. Geology, 16: 848–851.

Wernicke, B. and Burchfiel, B.C., 1982. Modes of extensional tectonics. J. Struct. Geol., 4: 105–115.

White, D.J., Easton, R.M., Culshaw, N.G., Milkereit, B., Forsyth, D.A., Carr, S., Green, A.G. and Davidson, A., 1994. Seismic images of the Grenville Orogen in Ontario. Can. J. Earth Sci., 31: 293–307.

Wolff, J.M., 1982. Geology of the Long Lake area, Lennox and Addington and Frontenac counties. Ont. Geol. Surv. Rep., 216, 76 pp.

Wolff, J.M., 1985. Geology of the Sharbot Lake area, Frontenac and Lanark counties, southeastern Ontario. Ont. Geol. Surv. Rep., 228, 70 pp.

Zelt, C.A., Forsyth, D.A., Milkereit, B., White, D.J., Asudeh, I. and Easton, R.M., 1994. Seismic structure of the Central Metasedimentary Belt, southern Grenville Province. Can. J. Earth Sci., 31: 243–254.